Journal of Nonlinear Modeling and Analysis
Volume 7, Number 6, December 2025, 2048–2077
https://journal.global-sci.org/jnma
DOI:10.12150/jnma.2025.2048

Mathematical Analysis of COVID-19 Fractional Model Incorporating Vaccination, Quarantine and Isolation Measures

Remigius Okeke Aja[1], William Atokolo[2,†], David Omale[2], Godwin Onuche Acheneje[2], Jeremiah Amos[2] and Agbata Celestine Benedict[3]

Abstract This study investigates the role of vaccination, quarantine, and isolation in controlling the spread of COVID-19 using a fractional-order mathematical model. The model consists of six non-linear fractional-order differential equations in the Caputo sense. Stability analysis is conducted using the Ulam-Hyers and modified Ulam-Hyers criteria, and the existence and uniqueness of solutions are explored with the Schauder and Banach fixed-point theorems. The model's dynamical behavior is analyzed using the fractional Euler method. Dimensional consistency is maintained during the fractionalization process, distinguishing this study from many contemporary investigations. The results show that increasing vaccination rates, improving quarantine protocols, and enhancing isolation facilities are effective strategies for reducing COVID-19 transmission.

Keywords Vaccination, quarantined, isolation, existence and uniqueness, Ulam-Hyers stability, Schauder and Banach fixed point theorem

MSC(2010) 00A71

1. Introduction

Since the start of March 2020 till now, the coronavirus has been causing new infections; as of right now, 1,575,186 cases have been reported in Pakistan [1, 2]. Of the overall number of cases, 98% of the infected people have recovered, while 30,631 deaths have been reported, making up 2% of the total cases. There have been several waves of coronavirus infection since March 2020; the most recent wave, or sixth wave, was seen between May–September 2022 [2]. If we examine the data provided in [2], we can see that there were multiple infections in the past, and that the number of infections has steadily declined in the most recent wave. One of the causes is that, in the past, people were ignorant of the problem and vaccines were not available on the market. Vaccination is a helpful method of defending people from illness. The coronavirus infection posed a significant threat to global health

[†]the corresponding author.
Email address:williamsatokolo@gmail.com(William Atokolo)
[1]Department of Mathematics, Michael Okpara University of Agriculture, Umudike, 440101, Nigeria
[2]Department of Mathematical Sciences, Prince Abubakar Audu University, Anyigba, 272102, Nigeria
[3]Department of Mathematics and Statistics, Confluence University of Science and Technology, Osara, 264103, Nigeria

because there was no known cure or preventative measure, despite the availability of immunizations. A notable reduction in the number of coronavirus infection cases has occurred thanks to the efforts of scientists and researchers developing vaccinations. The following list of mathematical models make use of the control strategies: [3, 4]. A model for coronavirus infection incorporating control methods was shown in [3]. Several control mechanisms were considered in the research on the coronavirus, using the fractional-order model presented in [4]. There are several varieties of coronavirus vaccines on the market, including those made by Moderna, Pfizer, Johnson and Johnson, China, and others [5]. Notably, there is still a declining vaccination rate despite the fact that none of the vaccinations created to date is 100% effective. As a result, a disclaimer regarding vaccinations has been included in the most recent vaccine campaigns. It is impossible to develop vaccinations against coronavirus infection in certain parts of the world's less developed nations due to the lack of financial resources. One to ten people have been immunized in each of the 70 low-income nations in the world [6]. International organizations are working to reduce the coronavirus cases by distributing vaccinations equally.

It is important to emphasize that the unequal distribution of vaccinations cannot be corrected quickly, necessitating the investigation of more realistic immunization rates. Vaccines are thought to be the most effective means of controlling the elimination of disease, but their availability is restricted and influenced by a number of factors during the implementation process. Quarantining the unconfirmed cases of COVID-19 and isolating the confirmed cases for treatment are also effective in controlling the spread of COVID-19 in a population. International researchers working on vaccine methods have contributed valuable written resources to the literature. For instance, the authors of [6] researched the dynamics of epidemic diseases and created vaccination regimens for both single- and double-dose vaccinations. The authors of [7] formulated a vaccination model that took tactics for treatment and vaccine saturation into account. The topic of disease-containing vaccines and the impact of media campaigns was examined in [8]. In [9], the study of the vaccination model with subsequent infection following vaccination coverage and immunization was presented. The effects of therapy and vaccination on the coronavirus were investigated in [10]. The impact of vaccine methods on the eradication of disease and the availability of vaccines were discussed in [11–13]. A number of mathematical models were discussed in [14, 15] that study the bifurcation and local and global asymptotic dynamics of the coronavirus epidemic. A detailed discussion of the vaccination model including its efficiency and impact may be found in [16]. The literature has established mathematical models with integer and non-integer orders to comprehend infectious diseases, including COVID-19 specifically [17–19]. As an illustration, a model that uses actual data was developed and examined in [20]. A mathematical model was presented in [21] based on the distributions of the instances with asymptomatic and symptomatic compartments. In [22], the coronavirus treatment model was covered. The coronavirus vaccination model, including its defense mechanisms, was displayed in [23]. Martinez-Guerra and Flores-Flores [24] discussed the COVID-19 algorithm that is used to find undetected cases. In [25], a non-integer method for coronavirus analysis using actual cases from Pakistan was investigated. In order to comprehend the new Omicron variant, the SARS-CoV-2 formulation with fractional derivative was shown in [26].

A stability study and discussion of the second coronavirus infection wave was examined in [27]. A fractional-order model was used in [28] to analyze the coro-

navirus cases reported in India. The co-infection of COVID-19 and Monkeypox diseases was analyzed in [29] using the Laplace Adomian Decomposition Method. Further related uses of fractional calculus were demonstrated in [30–33]. Neural network dynamics was covered in [30]. The IIR filter was employed by the authors in [31] to obtain solutions for fractional-order equations related to grid-tied inverters. In [32], the dynamics of the prey-predator system were examined, and the fractional derivative was used for analysis. The Fractional Step-Down Oscillator system was analyzed numerically in [33]. In [34], the dynamics of cholera under a fractional differential equation framework was examined. A study on the kinetics of the coronavirus spread under fractional calculus was conducted in [35]. Okyere et al. [36] illustrated the dynamics of Monkeypox disease using arbitrary calculus. Fractional mathematical models of the Zika virus and Lassa fever were also presented in [37, 38], where the Laplace Adomian Decomposition Method and the Adams-Bashforth-Moulton method were applied to obtain approximate solutions for the formulated systems. Akter et al. [39] combined fractional-order derivatives with evolutionary game theory to study epidemic dynamics with diminishing immunity, demonstrating that integrating vaccination, personal protection, and quarantine significantly reduces disease spread. Ullah & Kabir [40] employed a fractional-order approach to model behavioral responses during the monkeypox epidemic, highlighting the impact of quarantine policies on disease mitigation and peak delay while emphasizing strict behavioral interventions in outbreak reduction. Ullah et al. [41] proposed a non-singular fractional-order logistic growth model for population forecasting in Bangladesh, offering a novel formal approach using adjusted census data to enhance national planning and development strategies. Ullah et al. [42] analyzed vaccination strategies with a fractional-order epidemic model, using an evolutionary game approach to explore dynamic vaccination responses and showcasing the effectiveness of game-theoretical frameworks in controlling disease spread. Ullah et al. [43] developed a modified epidemic model using deterministic, heterogeneous, and fractional-order approaches to analyze vaccination and lock down strategies. Their findings offer insights for effective epidemic management. Parsamanesh and Erfanian [44] did an innovative SIS epidemic model that incorporated recruitment, mortality, and vaccination strategies. They demonstrated how mathematical techniques could provide deeper insights into epidemic transmission through comprehensive equilibria and stability analysis, offering a nuanced understanding of population dynamics. Liu et al. [45] advanced coronavirus transmission understanding through a fractional calculus approach, reformulating epidemic models using the Caputo operator. They implemented nonlinear least square parameter estimation and advanced numerical schemes, providing a sophisticated framework for interpreting pandemic spread mechanisms. Bachar et al. [46] developed a sophisticated nonautonomous COVID-19 model featuring eight time-dependent compartments that integrated low-risk and high-risk population dynamics. They distinguished their research by differentiating between diagnosed and undiagnosed infected individuals, performing detailed parameter estimations and epidemic persistence analysis. Parsamanesh and Erfanian [47] introduced a discrete-time SIS epidemic model with vaccination, focusing on comprehensive model stability analysis. They explored complex bifurcation dynamics including fold, flip, and Neimark-Sacker bifurcations, and used numerical simulations to verify theoretical results. The study provided deep insights into the model's equilibria, basic reproduction number, and solution positivity conditions through advanced mathematical tech-

niques. Chahkand et al. [48] formulated a SEIaIsQRS epidemic model representing advanced numerical method sophistication. They developed a six-compartment COVID-19 dynamic model that proved solution positivity, calculated reproduction numbers, and applied center manifold theorem analysis to capture complex epidemic transmission dynamics. In this current study, we introduce a mathematical model with fractional orders to explore how vaccination, quarantine, and isolation impact the spread of COVID-19. We utilized the fractional Euler method to approximate solutions for the model. The well-known Schauder and Banach fixed point theorems were used to investigate the existence and uniqueness of the model solution. Some limitations of these methods are that a function being a weak contraction does not always guarantee the existence of a fixed point [49], and the Schauder fixed point theorem depends on the operator's compactness, with an operator being considered compact only if it is continuous and maps bounded subsets into relatively compact sets [50]. Also, the Ulam-Hyers stability of the suggested model, which is considered essential for determining the approximate solutions of models, has been examined. However, this method also has some weaknesses, which include that the infimum of the set of all Ulam-Hyers stability constants may be the only Ulam-Hyers stability constant [51] and the Ulam stability for a system can only be studied for those which satisfy identical compatibility conditions [52]. Despite extensive studies on COVID-19 mathematical models and transmission dynamics, limited research has incorporated vaccination, quarantine, and isolation of the infected as control strategies within a fractional calculus framework. By utilizing the fractional Euler method to approximate the solution of the proposed model, our work seeks to address this gap and provide valuable insights into effective strategies for controlling COVID-19 transmission. The following is the arrangement of the work: Section (1) contains the COVID-19 background and preliminaries on fractional calculus. Section (2) contains the model formulation for both integer- and non-integer-order cases. In Section (3), we discuss the existence and uniqueness of the model using the Schauder and Banach fixed-point theorems. Section (4) provides the system's stability analysis using the Ulam-Hyers and generalized Ulam-Hyers criteria for stability. We equally present an effective numerical scheme called the fractional Euler method for determining the approximate solutions of the model along with its simulations. Section (5) contains the concluding remark for our study.

1.1. Fractional calculus preliminaries

Definition 1.1. [53] If the fractional order $\Lambda > 0$ and $y \in L^{'}([0,a],R)$ where $[0,a] \subset R_{+}$, We now define the fractional integral in the sense of Riemann-Liouville of order Λ for a function y as follows

$$I_t^{\Lambda} y = \frac{1}{\lceil \Lambda} \int_0^t (t-\lambda)^{\Lambda-1} y(\lambda)\, d\lambda, \lambda > 0,$$

where $\lceil \Lambda$ is defined as the gamma function as follows:

$$\lceil \Lambda = \int_0^{\infty} \lambda^{\Lambda-1} e^{-\lambda} d\lambda. \tag{1.1}$$

Definition 1.2. [53] The Caputo fractional derivative of order Λ for a function y is defined as equation (1.2) provided that $m-1<\Lambda<m, m\in N$ and $y\in C^m[0,a]$.

$$ {}^{C}D_t^{\Lambda}y=\frac{1}{\left|\overline{(m-\Lambda)}\right.}\int_0^t(t-\lambda)^{m-\Lambda-1}y^m(\lambda)\,d\lambda, t>0. \tag{1.2}$$

Lemma 1.1. *[53] If $Re(\lambda)>0$, $m=[Re(\Lambda)]+1$ and $y\in BC^m(0,a)$. Therefore,*

$$ \left({}^{\Lambda}I_t^{C}D_t^{\Lambda}y\right)=y(t)-\sum_{n=1}^{k}\frac{(D_t^n)\,t}{n!}t^n. \tag{1.3}$$

When $0<\Lambda\leq 1$, we have that,

$$ \left({}^{\Lambda}I_t^{C}D_t^{\Lambda}y\right)=y(t)-y_0. \tag{1.4}$$

2. Mathematical model formulation

In this current study, we propose a deterministic $SEVQI_TR$ model for the transmission dynamics and control of COVID-19. We divide the total human population into six compartments: susceptible class S, exposed class E, vaccinated class V, quarantined class Q, infected but isolated for treatment class I_T, and recovered class R. The model formulation is as follows:

Susceptible Class, S is recruited at the rate of θ. The class decreases as a result of natural death at the rate ω and also due to the proportion of individuals being vaccinated at the rate τ_1. The class also decreases due to the proportion of susceptible individuals who become infected with the virus through contact with the exposed class at the rate ϕ_1 and with the infected but isolated for treatment class at the rate ϕ_2. This population grows as a result of the progression of recovered individuals losing immunity and becoming susceptible again at the rate γ_3. The waning of vaccine-induced immunity at the rate τ_2, as well as the confirmation of quarantined individuals as being COVID-19-free at the rate α_4, also increases the susceptible population. Although vaccine efficacy is not explicitly included, it is indirectly captured in τ_2, which reflects the waning of immunity and the potential failure of vaccination over time. The dynamics of this class are therefore formulated as follows:

$$ \frac{dS}{dt}=\theta-(\phi_1E+\phi_2I_T)S+\alpha_4Q+\tau_2V+\gamma_3R-(\tau_1+\omega)S. $$

Exposed Class, E increases as individuals progress into the class due to new infections occurring at the rates ϕ_1 and ϕ_2. The population decreases as a result of the progression of exposed individuals who become fully infectious and are therefore isolated for treatment at the rate α_1. Additionally, it decreases because a proportion of exposed individuals are quarantined for diagnosis at the rate α_2. Finally, the class also decreases due to natural death at the rate ω. The dynamics of this class are therefore formulated as follows:

$$ \frac{dE}{dt}=(\phi_1E+\phi_2I_T)S-(\alpha_1+\alpha_2+\omega)E. $$

Vaccinated Class, V increases as susceptible individuals are vaccinated at the rate τ_1. The population of the vaccinated decreases due to individuals transitioning back to the susceptible class as a result of vaccine failure or waning immunity, represented by the rate τ_2. This rate indirectly captures the vaccine's efficacy and durability. Although the vaccine is not yet perfect, τ_2 indirectly captures its limitations. A proportion of the vaccinated individuals progress to the recovered class based on immunity development. Finally, the class also decreases due to natural death at the rate ω. The dynamics of this population are therefore presented as follows:

$$\frac{dV}{dt} = \tau_1 S - (\tau_2 + \gamma_2 + \omega) V.$$

Quarantined Class, Q increases due to the transfer of unconfirmed cases from the exposed class to the quarantined class for diagnosis at the rate α_2. The class decreases as individuals confirmed to be COVID-19 negative after diagnosis return to the susceptible class at the rate α_4. Secondly, it decreases as those confirmed positive with clinical symptoms of COVID-19 are moved to treatment in isolation centers at the rate α_3. Finally, the class decreases due to natural deaths occurring at the rate ω. The dynamics for the class are formulated as follows:

$$\frac{dQ}{dt} = \alpha_2 E - (\alpha_3 + \alpha_4 + \omega) Q.$$

Infected but Isolated for Treatment Class, I_T increases due to the movement of confirmed COVID-19 cases from the quarantined class and the progression of fully infectious individuals from the exposed class to isolation centers for treatment. The class decreases as individuals recover after treatment at the rate γ_1 and as a result of deaths caused by the disease at the rate δ. It also decreases due to natural deaths occurring at the rate ω. The dynamics of this class are formulated as follows:

$$\frac{dI_T}{dt} = \alpha_1 E + \alpha_3 Q - (\gamma_1 + \delta + \omega) I_T.$$

Recovered Class, R grows as individuals recover after treatment in the isolation center at the rate γ_1. Additionally, the population increases due to vaccinated individuals transitioning to the recovered class after successful immunization. The recovered class decreases as a result of the loss of immunity in recovered individuals, causing them to re-enter the susceptible class at the rate γ_3. Finally, the population in this class reduces due to natural deaths occurring at the rate ω. The dynamics of this class are formulated as follows:

$$\frac{dR}{dt} = \gamma_1 I_T + \gamma_2 V - (\gamma_3 + \omega) R.$$

The schematic representation of our model formulation is illustrated in Figure 1.

Based on the model assumptions, we present the mathematical model for COVID-19 as follows:

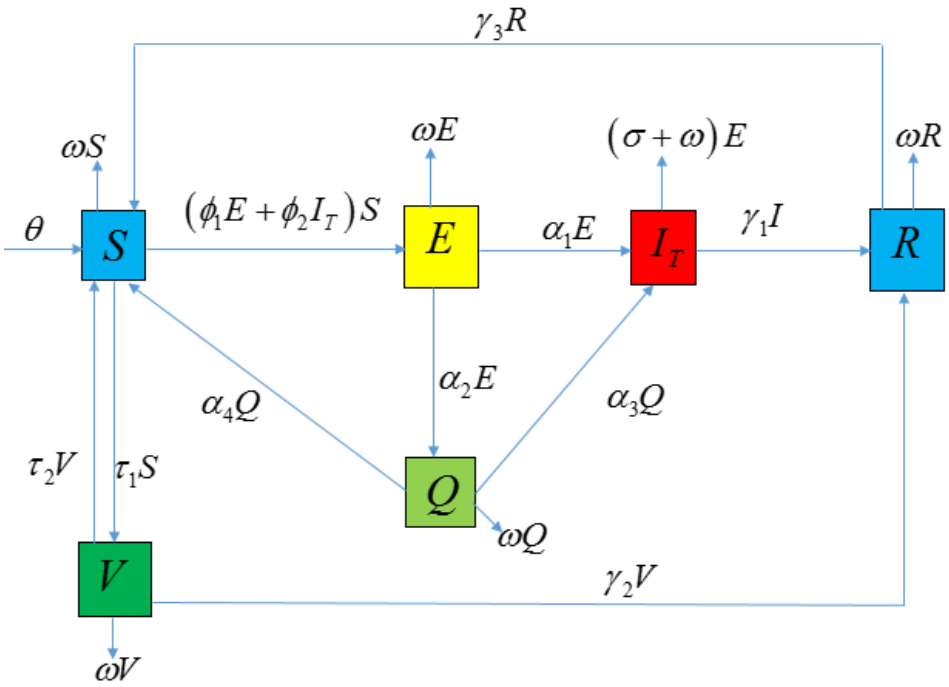

Figure 1. Flow diagram for the COVID-19 model

$$\left.\begin{aligned}
\tfrac{dS}{dt} &= \theta - (\phi_1 E + \phi_2 I_T)\, S \\
&\quad + \alpha_4 Q + \tau_2 V + \gamma_3 R - (\tau_1 + \omega)\, S, \\
\tfrac{dE}{dt} &= (\phi_1 E + \phi_2 I_T)\, S - (\alpha_1 + \alpha_2 + \omega)\, E, \\
\tfrac{dV}{dt} &= \tau_1 S - (\tau_2 + \gamma_2 + \omega)\, V, \\
\tfrac{dQ}{dt} &= \alpha_2 E - (\alpha_3 + \alpha_4 + \omega)\, Q, \\
\tfrac{dI_T}{dt} &= \alpha_1 E + \alpha_3 Q - (\gamma_1 + \delta + \omega)\, I_T, \\
\tfrac{dR}{dt} &= \gamma_1 I_T + \gamma_2 V - (\gamma_3 + \omega)\, R.
\end{aligned}\right\} \tag{2.1}$$

Extending the integer model represented in equation (2.1), we now present a new COVID-19 model using Caputo fractional operator in equation (2.2) below:

$$\left.\begin{aligned}
{}^{C}D_t^{\Lambda} S &= \theta - (\phi_1 E + \phi_2 I_T)\, S \\
&\quad + \alpha_4 Q + \tau_2 V + \gamma_3 R - (\tau_1 + \omega)\, S, \\
{}^{C}D_t^{\Lambda} E &= (\phi_1 E + \phi_2 I_T)\, S - (\alpha_1 + \alpha_2 + \omega)\, E, \\
{}^{C}D_t^{\Lambda} V &= \tau_1 S - (\tau_2 + \gamma_2 + \omega)\, V, \\
{}^{C}D_t^{\Lambda} Q &= \alpha_2 E - (\alpha_3 + \alpha_4 + \omega)\, Q, \\
{}^{C}D_t^{\Lambda} I_T &= \alpha_1 E + \alpha_3 Q - (\gamma_1 + \delta + \omega)\, I_T, \\
{}^{C}D_t^{\Lambda} R &= \gamma_1 I_T + \gamma_2 V - (\gamma_3 + \omega)\, R.
\end{aligned}\right\} \tag{2.2}$$

The description of the model variables and parameters is presented in Tables (1 and 2)

Variables (Parameters)	**Description**
S	Susceptible individuals
E	Exposed individuals
V	Vaccinated individuals
Q	Quarantined individuals
I_T	Infected but isolated for treatment
R	Recovered individuals
θ	Recruitment rate
τ_1	Vaccination rate
τ_2	Wanning rate of vaccine
ϕ_1	Contact rate between E and S
ϕ_2	Contact rate between I_T and S
ω	Natural death rate
α_4	Rate at which the quarantined becomes susceptible
α_2	Quarantine rate of exposed
α_1	Rate at which infected are isolated for treatment

Table 1. Description of Variables and Parameters

Parameters	Description
α_3	Rate at which the quarantined are isolated are treatment
γ_1	Recovery rate due to treatment
γ_2	Rate at which the vaccinated are removed
σ	COVID-19 induced death rate
γ_3	Rate at which the recovered becomes susceptible

Table 2. Description of Parameters

3. Existence and uniqueness of proposed model solution

One of the most important areas in the theory of fractional order differential equations is the notion of the existence and uniqueness of solutions. The theory has gained popularity among scholars like those presented in [54–59]. Using fixed point theorems, we address the existence and uniqueness of solutions to the suggested model in this section. We apply the following configuration to our model in (2.2). The fractional model (2.2) can be written as follows:

$$\left.\begin{aligned} {}^{C}D_t^{\Lambda} S &= \psi_1(t, S, E, V, I_T, R), \\ {}^{C}D_t^{\Lambda} E &= \psi_2(t, S, E, V, I_T, R), \\ {}^{C}D_t^{\Lambda} V &= \psi_3(t, S, E, V, I_T, R), \\ {}^{C}D_t^{\Lambda} Q &= \psi_4(t, S, E, V, I_T, R), \\ {}^{C}D_t^{\Lambda} I_T &= \psi_5(t, S, E, V, I_T, R), \\ {}^{C}D_t^{\Lambda} R &= \psi_6(t, S, E, V, I_T, R). \end{aligned}\right\} \tag{3.1}$$

where

$$\left.\begin{aligned} \psi_1(t, S, E, V, I_T, R) &= \theta - (\phi_1 E + \phi_2 I_T) S + \alpha_4 Q + \tau_2 V + \gamma_3 R \\ &\quad - (\tau_1 + \omega) S, \\ \psi_2(t, S, E, V, I_T, R) &= (\phi_1 E + \phi_2 I_T) S - (\alpha_1 + \alpha_2 + \omega) E, \\ \psi_3(t, S, E, V, I_T, R) &= \tau_1 S - (\tau_2 + \gamma_2 + \omega) V, \\ \psi_4(t, S, E, V, I_T, R) &= \alpha_2 E - (\alpha_3 + \alpha_4 + \omega) Q, \\ \psi_5(t, S, E, V, I_T, R) &= \alpha_1 E + \alpha_3 Q - (\gamma_1 + \delta + \omega) I_T, \\ \psi_6(t, S, E, V, I_T, R) &= \gamma_1 I_T + \gamma_2 V - (\gamma_3 + \omega) R. \end{aligned}\right\} \tag{3.2}$$

We can therefore simply present model (2.2) as:

$$\left.\begin{aligned} {}^{C}D_t^{\Lambda} \psi(t) &= L(t, \psi(t)), \mathrm{t} \in \mathrm{I} = [0, a], 0 < \gamma \leq 1, \\ \psi(0) &= \psi_0 \geq 0, \end{aligned}\right\} \tag{3.3}$$

So that the condition presented in (3.4) is satisfied where $(...)^T$ implies transpose functional.

$$\left.\begin{aligned}&\psi(t)=(S,E,V,Q,I_T,R)^T,\\&\psi(0)=(S_0,E_0,V_0,Q_0,I_{T0},R_0)^T,\\&\chi(t,\psi(t)),i=1,...,6.\end{aligned}\right\} \tag{3.4}$$

Using Lemma 1.1, our model (2.2) is the same as system (3.3) integral characterization which is presented in equation (3.5).

$$\left.\begin{aligned}&\psi(t)=\psi_0+I_t^{\Lambda}\chi(t,\psi(t)),\\&\psi(t)=\psi_0+\frac{1}{\lceil\Lambda}\int_0^t(t-\lambda)^{\Lambda-1}\chi(\lambda,\psi(\lambda))\,d\lambda.\end{aligned}\right\} \tag{3.5}$$

If $B=C([0,a],R)$ represents the Banach space for all functions that are continuous from $[0,a]$ empowered with the defined norm presented in (3.6) below:

$$\|\psi\|_B=\sup_{t\in I}|\psi(t)|, \tag{3.6}$$

where

$$|\psi(t)|=|S(t)|+|E(t)|+|V(t)|+|Q(t)|+|I_T(t)|+|R(t)|,$$

$$S,E,V,Q,I_T,R\in\subset([0,a]).$$

Theorem 3.1. *Assume that the function $\chi\in([I,R])$ maps a bounded subset of $I\times R^6$ into a compact subset of R and that a constant M_I exists such that*

(1) $|\chi(t,\psi_1(t))-\chi(t,\psi_2(t))|\leq M_\chi|\psi_1(t)-\psi_2(t)|$ for all $t\in I$ so that each $\psi_1,\psi_2\in\subset([I,R])$.

Therefore, model (2.2) which is same as system (3.3) has a unique solution whenever $KM_\chi<1$, where $k=\frac{a^\Lambda}{\lceil(\Lambda+1)}$.

Proof. Imagine an operator $L:B\to B$ defined by

$$(B\psi)(t)=\psi_0+\frac{1}{\lceil\Lambda}\int_0^t(t-\lambda)^{\Lambda-1}\chi(t,\psi(\lambda))\,d\lambda.$$

The unique solution of our model (3.3) is the fixed point of which the operator is also well defined.

If $\sup_{t\in I}\|\chi(t,0)\|=N_1$ and $l\geq\|\psi_0\|+\tau N_1$, then, to this end, it is sufficient to show that $BQ_1\subset Q_1$, where the set $Q_1=\{\psi\in B:\|\psi\|\leq r\}$ is convex and closed so that for any $\psi\in Q_l$ we have

$$|(B\psi)|\leq|\psi_0|+\frac{1}{\lceil\overline{(\Lambda)}}\int_0^t(t-\lambda)^{\Lambda-1}|\chi(\lambda,\psi(\lambda))|\,d\lambda$$

$$
\begin{aligned}
&\leq \frac{1}{\left|\overline{(\Lambda)}\right.} \int_0^t (t-\lambda)^{\Lambda-1} \left[\left|\chi\left(\lambda, \psi\left(\lambda\right)\right) - \chi\left(\lambda, 0\right)\right| + \left|\chi\left(\lambda, 0\right)\right|\right] d\lambda \\
&\leq \psi_0 + \frac{\left(M_\chi l + N_1\right)}{\left|\overline{\Lambda}\right.} \int_0^t (t-\lambda)^{\Lambda-1} d\lambda \\
&\leq \psi_0 + \frac{\left(M_\chi l + N_1\right)}{\left|\overline{\Lambda+1}\right.} a^\Lambda \\
&\leq \psi_0 + \frac{\tau\left(M_\chi l + N_1\right)}{\left|\overline{\Lambda+1}\right.} a^\Lambda \\
&\leq \psi_0 + \tau\left(M_\chi l + N_1\right) \\
&\leq l. \qquad (3.7)
\end{aligned}
$$

Similarly, given any $\psi_1, \psi_2 \in B$, we also have that

$$
\begin{aligned}
\left|\left(B\psi_1\right)(t) - \left(B\psi_2\right)(t)\right| &\leq \frac{1}{\left|\overline{(\Lambda)}\right.} \int_0^t (t-\lambda)^{\Lambda-1} \left|\chi\left(\lambda, \psi_1\left(t\right) - \chi\left(\lambda, \psi_2\left(\lambda\right)\right)\right)\right| d\left(\lambda\right) \\
&\leq \frac{M_\chi}{\left|\overline{(\Lambda)}\right.} \int_0^t (t-\lambda)^{\Lambda-1} \left|\psi_1\left(\lambda\right) - \psi_2\left(\lambda\right)\right| d\left(\lambda\right). \qquad (3.8)
\end{aligned}
$$

Equation (3.8) means $\left\|\left(B\psi_1\right) - \left(\beta\psi_2\right)\right\| \leq \tau M_\chi \left\|\psi_1 - \psi_2\right\|$.

Therefore our model (2.2) has a unique solution as a result of the Banach contraction principle.

Recall that the COVID-19 model (2.2) is the same as system (3.3). Applying the Schaunder fixed point theorem concept, we investigate the existence of our model solution. The assumption (2) below is required.

(2) If there exist $a_1, a_2 \in B$ then

$$\left|\chi\left(t, \psi\left(t\right)\right)\right| \leq a_1\left(t\right) + a_2\left(t\right)$$

for any $\psi \in B, t \in I$, such that

$$
\begin{aligned}
a_1^* &= \sup_{t \in I} \left|a_1\left(t\right)\right|, \\
a_2^* &= \sup_{t \in I} \left|a_2\left(t\right)\right| < 1.
\end{aligned}
$$

□

Lemma 3.1. *From equation (3.7) the defined operator B is continuously completed.*

Proof. Clearly, the continuity of χ as a function defines the continuity of B as an operator.

Then for any $\psi \in Q_l$ where Q_l is expressed above, we now have

$$
\begin{aligned}
\left|\left(B\psi\right)(t)\right| &= \left|\psi_0 + \frac{1}{\left|\overline{(\Lambda)}\right.} \int_0^t (t-\lambda)^{\Lambda-1} \chi\left(\lambda, \psi\left(\lambda\right)\right) d\lambda\right|, \\
&\leq \left\|\psi_0\right\| + \frac{1}{\left|\overline{(\Lambda)}\right.} \int_0^t (t-\lambda)^{\Lambda-1} \left|\chi\left(\lambda, \psi\left(\lambda\right)\right)\right| d\lambda.
\end{aligned}
$$

□

$$\begin{aligned}|(B\psi)(t)| &\leq \|\psi_0\| + \frac{(a_1^* + a_2^* \|\psi\|)}{\left|\overline{(\Lambda)}\right.} \int_0^t (t-\lambda)^{\Lambda-1} d\lambda \\ &\leq \|\psi_0\| + \frac{(a_1^* + a_2^* \|\psi\|)}{\left|\overline{(\Lambda+1)}\right.} a^{\Lambda} \\ &= \|\psi_0\| + \tau (a_1^* + a_2^* \|\psi\|) \\ &\Rightarrow |(B\psi)(t)| < +\infty.\end{aligned} \tag{3.9}$$

This implies that B as an operator is bounded uniformly.
To show that the operator B is equicontinuous, we assume that,

$$\sup_{(t,\psi)\in I\times P_l} |\chi(t,\psi(t))| = \chi^*.$$

Therefore, for any $t_1, t_2 \in I$, whenever $t_1 \leq t_2$, it gives

$$\begin{aligned}|(B\psi)\, t_2 - (B\psi)(t_1)| =& \frac{1}{\left|\overline{(\Lambda)}\right.} \left| \begin{matrix} \int_0^t \left[(t_2-\lambda)^{\Lambda-1} - (t_1-\lambda)^{\Lambda-1}\right] \chi(\lambda,\psi(\lambda)) d\lambda \\ + \int_{t_1}^{t_2} (t_2-\lambda)^{\Lambda-1} \chi(\lambda,\psi(\tau)) d\lambda \end{matrix} \right| \\ \leq& \frac{\chi^*}{\left|\overline{(\Lambda)}\right.} \left[2(t_2-t_1)^{\Lambda} + \left(t_2^{\Lambda} - t_1^{\Lambda}\right)\right] \\ & |(B\psi)(t_2) - (B\psi)(t_1)| \to P\end{aligned} \tag{3.10}$$

We therefore conclude that operator B is equicontinuous at the same time relatively compact on Q_χ.

Operator B is completely continuous as a result of Arzela-Ascoli theorem following the equicontinuity of operator B which is relatively compact on Q_χ.

Theorem 3.2. *If $\chi : I \times R^6 \to R$ is continuous which also satisfies assumption (2), then system (3.3) which is the same as model (2.2) has at least one single solution.*

Proof. Assume that a set (V) is defined as

$$V = \{\psi \in E : \psi = (B\psi)(t), 0 < o < 1\}.$$

From Lemma 3.1, the operator $B : V \to E$ is expressed in equation (3.7) as an operator which is completely continuous. Then for any $\psi \in V$, using our assumption (2), we have that,

$$\begin{aligned}&|(\psi)(t)| = |o(B\psi)(t)| \\ &\leq |\psi_0| + \tfrac{1}{\left|\overline{(\Lambda)}\right.} \int_0^t (t-\lambda)^{\Lambda-1} |\chi(\lambda,\psi(\lambda))| d\lambda \\ &\leq \|\psi_0\| + \tfrac{(a_1^* + a_2^* \|\psi\|)}{\left|\overline{(\Lambda+1)}\right.} a^{\Lambda} \\ &= \|\psi_0\| + \tau (a_1^* + a_2^* \|\psi\|).\end{aligned}$$

Therefore,

$$|(\psi)(t)| < +\infty. \tag{3.11}$$

Thus, V is a bounded set. Therefore the operator B has at least one fixed point which happens to be the only solution of the COVID-19 model represented by equation (2.2).

□

4. Ulam-Hyers and generalized Ulam-Hyers stability results

The stability of the suggested model (2.2) in the Ulam-Hyers and generalized Ulam-Hyers sense is derived in this section. Ulam introduced the idea of Ulam stability [60, 61]. Subsequently, the above method was examined in a number of research works on fractional derivatives. Notable among them are those presented in [62–66]. Furthermore, we aim to use the generalized stability of the suggested model (2.2) and non-linear fractional analysis of Ulam-Hyers as stability is essential for determining approximate solutions of models like ours. Therefore, the definitions that follow are required.

$$\left|{}^{C}D_{t}^{\Lambda}\,\bar{\psi}(t) - \chi\left(t, \bar{\psi}(t)\right)\right| \leq \varepsilon, t \in I,$$

where,

$$\varepsilon = max\,(\varepsilon_i)^T, i = 1, ..., 6. \tag{4.1}$$

Definition 4.1. ([61]) Our suggested model (2.2) which is the same as (3.3) is Ulam-Hyers stable if there exists $S_\chi > 0$ such that for every $\varepsilon > 0$ and for each solution $\psi \in E$ of system (3.3), we have

$$\left|\bar{\psi}(t) - \psi(t)\right| \leq S_\chi \varepsilon, t \in I,$$

where $S_k = max\,(S_{\chi i})^T$

Definition 4.2. The system (3.3) which is the same as our model (2.2) is said to be stable in the sense of the generalized Ulam-Hyers if there exists $S_\chi > 0$ and a function $L_\chi : R_+ \to R_1$, that is continuous with $L_\chi(0) = 0$ such that for a single solution $\bar{\psi} \in E$ of system (4.1), there exists a solution $\psi \in E$ of model (4.1) such that

$$\left|\bar{\psi}(t) - \psi(t) \leq L_\chi \in, t \in I\right|,$$

where $L_\chi = max\,(L_\chi i)^T$.

Remark 4.1. A function $\bar{\psi} \in E$ is said to be a solution of system (4.1) if the function $C \in E$ exists with the characteristics given below

a) $|C(t)| \leq \varepsilon,\ C = \max(C_i)^T,\ t \in I$;

b) ${}^{C}D_{t}^{\Lambda}\bar{\psi}(t) = \chi(t, \bar{\psi}(t)) + C(t),\ t \in I.$

Lemma 4.1. *If $\bar{\psi} \in E$ as function that satisfies system (4.1), it therefore means that the inequality presented in (4.2) below is satisfied by ψ.*

$$\left|\bar{\psi}(t) - \bar{\psi}_0 - \frac{1}{\Gamma(\Lambda)}\int_0^t (t-\lambda)\,\chi\left(\lambda, \bar{\psi}(\lambda)\right) d\lambda\right| \leq \tau\varepsilon. \tag{4.2}$$

Proof. From remark (b) of remark (4.1),

$${}^{C}D_{t}^{\Lambda}\,\bar{\psi}(t) = \chi\left(t, \bar{\psi}(t)\right) + C(t).$$

From Lemma 1.1 also, we have that

$$\begin{aligned}\bar{\psi}(t) = \bar{\psi}_0 + \frac{1}{\Gamma(\Lambda)}\int_0^t (t-\lambda)^{\Lambda-1}\chi\left(\lambda, \bar{\psi}(t)\right) d\lambda \\ + \frac{1}{\Gamma(\Lambda)}\int_0^t (t-\lambda)^{\Lambda-1} C(\lambda)\, d\lambda.\end{aligned} \tag{4.3}$$

Also from remark (a) of remark (4.1), we now have,

$$\begin{aligned}&\left|\bar{\psi}(t) - \bar{\psi}_0 - \tfrac{1}{\Gamma(\Lambda)}\int_0^t (t-\lambda)^{\Lambda-1}\chi\left(\lambda, \bar{\psi}(\lambda)\, d\lambda\right)\right| \\ &\leq \tfrac{1}{\Gamma(\Lambda)}\int_0^t (t-\lambda)^{\Lambda-1}\left|C(\lambda)\right| d\lambda \\ &\leq \tau\varepsilon,\end{aligned} \tag{4.4}$$

which is the required result. □

Theorem 4.1. *Given that $\chi : I \times R^6$ is continuous for every $\psi \in E$ and if our assumption (1) of Theorem 3.1 holds for $1 - \tau M_{\chi} > 0$, then, systen (3.3) which is the same as model (2.2) is Ulam-Hyer and also in the sense of generalized Ulam-Hyers stable.*

Proof. If $\bar{\psi} \in E$ has a function that satisfies system (4.1) and secondly if $\psi \in E$ is a solution which is unique to system (3.3). Then, for any $\varepsilon > 0$ and $t \in I$, it follows from lemma (4.1) that

$$\begin{aligned}\left|\bar{\psi}(t) - \psi(t)\right| &= \max_{t\in I}\left|\bar{\psi}(t) - \psi_0 - \frac{1}{\Gamma(\Lambda)}\int_0^t (t-\lambda)^{\Lambda-1}\chi\left(\lambda, \psi(\lambda)\right) d\lambda\right| \\ &\leq \max_{t\in I}\left|\bar{\psi}(t) - \psi_0 - \frac{1}{\Gamma(\Lambda)}\int_0^t (t-\lambda)^{\Lambda-1}\chi\left(\lambda, \psi(\lambda)\right) d\lambda\right| \\ &\quad + \max_{t\in I}\frac{1}{\Gamma(\Lambda)}\int_0^t (t-\lambda)^{\Lambda-1}\left|\chi\left(\lambda, \bar{\psi}(\lambda)\right) - \chi\left(\lambda, \psi(\lambda)\right)\right| d\lambda\end{aligned}$$

$$\leq \left| \psi(t) - \bar{\psi}_0 - \frac{1}{\overline{|(\Lambda)}} \int_0^t (t-\lambda)^{\Lambda-1} \chi(\lambda, \psi(\lambda)) \, d\lambda \right|$$
$$+ \frac{M_\chi}{\overline{|(\Lambda)}} \int_0^t (t-\lambda)^{\Lambda-1} \left| \bar{\psi}(\lambda) - \psi(\lambda) \, d\lambda \right|$$

$$\left| \bar{\psi}(t) - \psi(t) \right| \leq \tau\varepsilon + \tau M_\chi \left| \bar{\psi}(t) - \psi(t) \right|.$$

Therefore, $\left\| \bar{\psi} - \psi \right\| \leq B_x \varepsilon$, where $B_\chi = \frac{\tau}{1-\tau M_\chi}$.

If $\sigma_\chi(B_\chi \varepsilon)$ so that $\sigma_\chi(0) = 0$, then we can conclude that the COVID-19 model suggested in (2.2) is both stable in the sense of Ulam-Hyers and generalized Ulam-Hyers.

□

4.1. Model numerical simulation

In this section, the fractional model of COVID-19 presented in (2.2) is simulated numerically using proposed methods in [67–69]. The method employed in [67–69] is stable conditionally, and they converge easily while maintaining solution accuracy. The fractional Euler method used in this present study is effective and efficient in finding approximate solutions to fractional order linear and non-linear systems of ordinary differential equation problems that arise in physics, mathematics, engineering and generally in the field of sciences.

Looking at a fractional order general Cauchy problem with an autonomous nature presented in (4.5) below:

$$\begin{aligned} &{}^{C}D_t^{\Lambda}(x(t)) = g(x(t)), \Lambda \in (0,1] \mathrm{t} \in [0,T], \\ &x(0) = x_0, \end{aligned} \tag{4.5}$$

where $x = (m, n, o, p) \in R_+^4$ is a real valued vector fraction that is continuous which also satisfies the Lipchitz criterion presented as:

$$\|g(x_1(t)) - g(x_2(t))\| \leq U \|x_1(t) - x_2(t)\|, \tag{4.6}$$

where U is a non-negative Lipschitz constant, we now have

$$x(t) = x_0 + I_t^{\Lambda} g(x(t)), t \in [0,T]. \tag{4.7}$$

I_t^T is the Riemann-Liouville fractional order integral operator. Consider an interval $[0,T]$, that is spaced equally with step size $C = 0.02 = \frac{T}{n}, n \in N$.

If we assume a_b as an approximation of $x(t)$ at $t = t_b$ for $b = 0, 1, 2, ...n$, we therefore present a numerical method for the Caputo fractional derivative operator model (2.2) in equation [25] below.

$$\left.\begin{aligned}
{}^{C}S_{x+1} &= d_0 + \tfrac{C^{\Lambda}}{\Gamma(\Lambda+1)} \sum_{k=0}^{x} \left((x-k+1)^{\Lambda} - (x-k)^{\Lambda}\right) \begin{pmatrix} \theta - (\phi_1 E + \phi_2 I_T)\, S \\ + \alpha_4 Q + \tau_2 V + \gamma_3 R - (\tau_1 + \omega)\, S \end{pmatrix}, \\
{}^{C}E_{x+1} &= e_0 + \tfrac{C^{\Lambda}}{\Gamma(\Lambda+1)} \sum_{k=0}^{x} \left((x-k+1)^{\Lambda} - (x-k)^{\Lambda}\right) \left((\phi_1 E + \phi_2 I_T)\, S - (\alpha_1 + \alpha_2 + \omega)\, E\right), \\
{}^{C}V_{x+1} &= f_0 + \tfrac{C^{\Lambda}}{\Gamma(\Lambda+1)} \sum_{k=0}^{x} \left((x-k+1)^{\Lambda} - (x-k)^{\Lambda}\right) \left(\tau_1 S - (\tau_2 + \gamma_2 + \omega)\, V\right), \\
{}^{C}Q_{x+1} &= g_0 + \tfrac{C^{\Lambda}}{\Gamma(\Lambda+1)} \sum_{k=0}^{x} \left((x-k+1)^{\Lambda} - (x-k)^{\Lambda}\right) \left(\alpha_2 E - (\alpha_3 + \alpha_4 + \omega)\, Q\right), \\
{}^{C}I_{Tx+1} &= i_0 + \tfrac{C^{\Lambda}}{\Gamma(\Lambda+1)} \sum_{k=0}^{x} \left((x-k+1)^{\Lambda} - (x-k)^{\Lambda}\right) \left(\alpha_1 E + \alpha_3 Q - (\gamma_1 + \delta + \omega)\, I_T\right), \\
{}^{C}R_{x+1} &= j_0 + \tfrac{C^{\Lambda}}{\Gamma(\Lambda+1)} \sum_{k=0}^{x} \left((x-k+1)^{\Lambda} - (x-k)^{\Lambda}\right) \left(\gamma_1 I_T + \gamma_2 V - (\gamma_3 + \omega)\, R\right).
\end{aligned}\right\} \tag{4.8}$$

Now using the fractional order Euler method in the sense of Caputo operator, we obtain numerical solutions of the approximate solutions presented in equation (4.8).

We consider the following initial conditions for the numerical simulations while the parameter values used are tabulated in Table (3)

$$S(0) = 1000,\ E(0) = 500,\ V(0) = 300,\ Q(0) = 200.$$

(Parameters)	**Values**	**Sources**
θ	400	[70]
τ_1	0.1	Estimated
τ_2	0.001	Estimated
ϕ_1	0.000018	[71]
ϕ_2	0.000017	[71]
ω	0.0096	[70]
α_4	0.0001	Estimated
α_2	0.05	[70]
α_1	0.04	Estimated
α_3	0.01	Estimated
γ_1	0.16979	[7]
γ_2	0.16979	[7]
σ	0.03275	[7]
γ_3	0.23	[27]

Table 3. Values of model parameters

4.2. Results and discussions

Figures (2(a), 2(b), 3(a), 3(b), 4(a), 4(b)) illustrate the dynamic interplay between the susceptible, exposed, vaccinated, quarantined, infected, and recovered populations under varying fractional orders (Λ). Notably, an increase in Λ corresponds

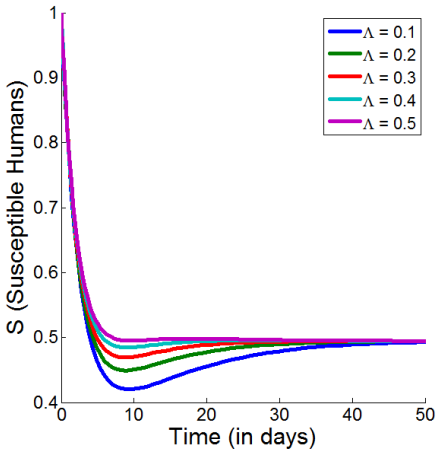

(a) Variation of Λ on Susceptible Humans

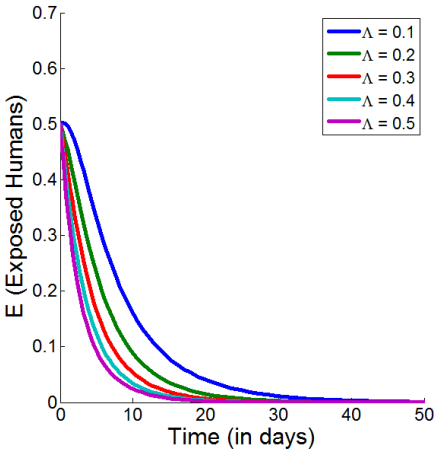

(b) Variation of Λ on Exposed Humans

Figure 2. Human Population

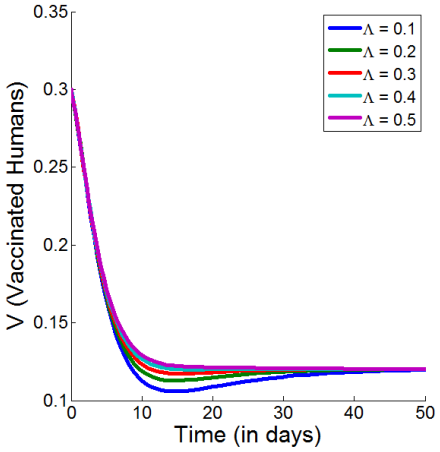

(a) Variation of Λ on Vaccinated Humans

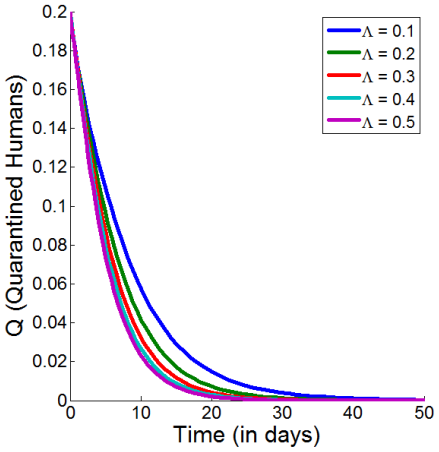

(b) Variation of Λ on Quarantined Humans

Figure 3. Human Population

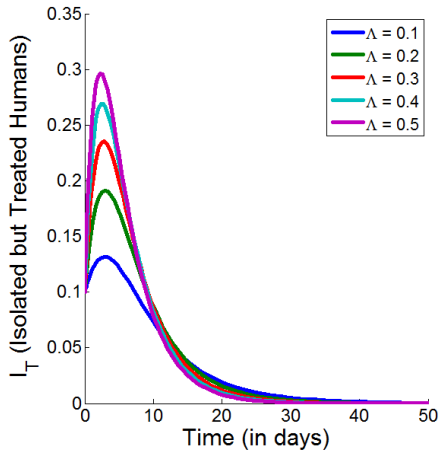

(a) Variation of Λ on Isolated Humans

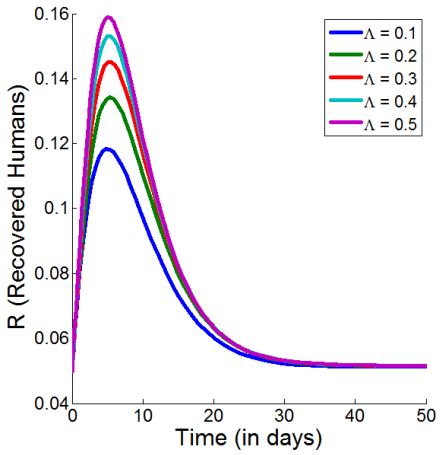

(b) Variation of Λ on Recovered Humans

Figure 4. Human Population

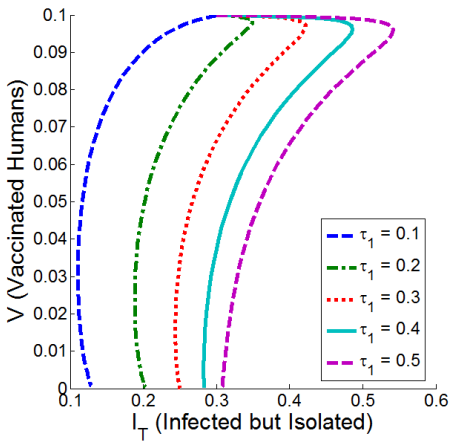

(a) Effect of the vaccinated class on the Isolated but treatment class

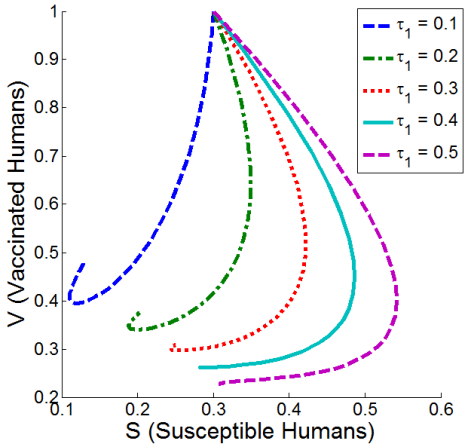

(b) Effect of the vaccinated class on the Susceptible class

Figure 5. Human Population

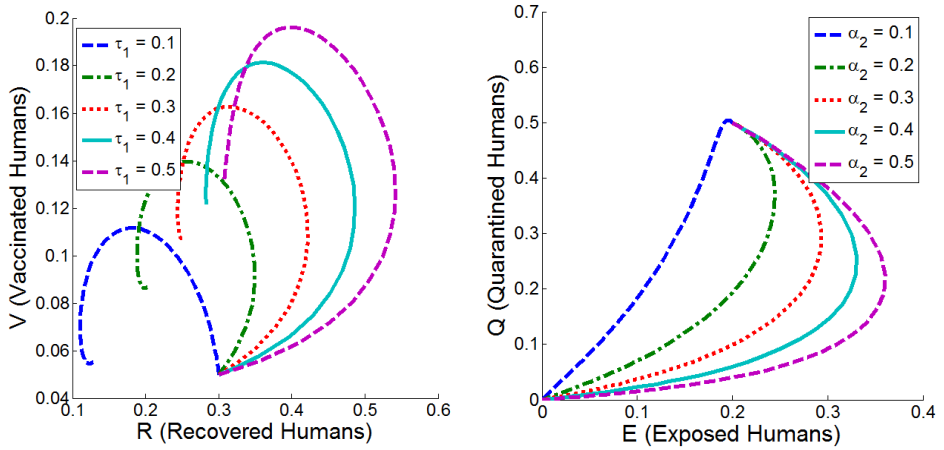

(a) Effect of the vaccinated class on the Recovered class

(b) Effect of the Quarantined class on the Exposed class

Figure 6. Human Population

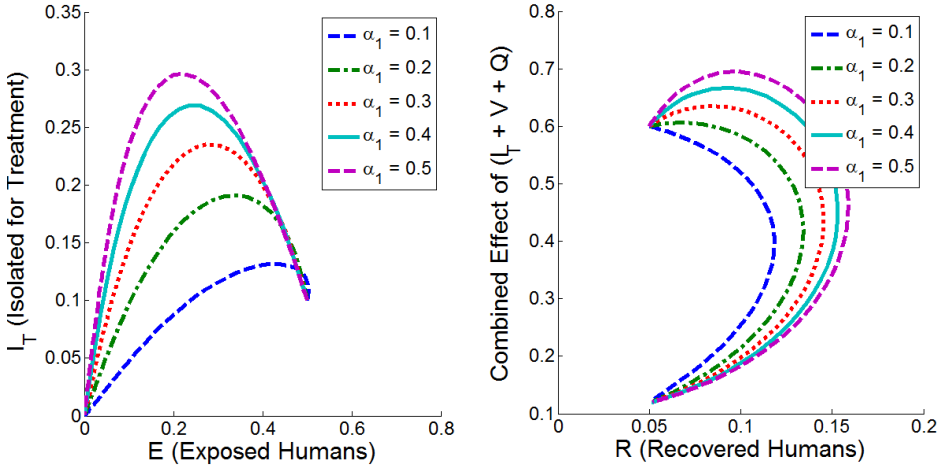

(a) Effect of the Isolated class on the Exposed class

(b) Combined Effect of the Isolated, Vaccinated and Quarantined classes on the Recovered class

Figure 7. Human Population

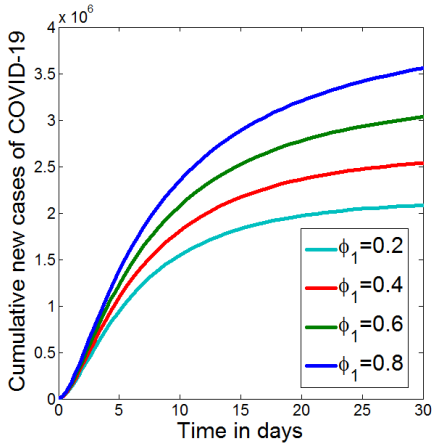

(a) Cumulative new cases of COVID-19

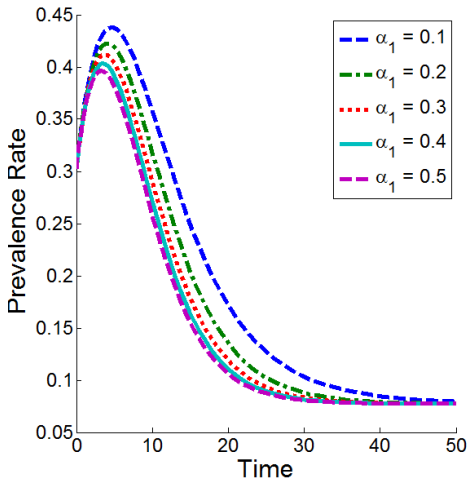

(b) Prevalence of COVID-19 in the Human population

Figure 8. Human Population

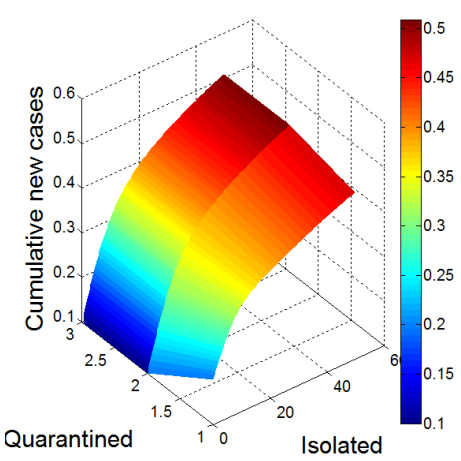

(a) Surface plot of the Quarantined and Isolated class on the Cumulative new cases of COVID-19

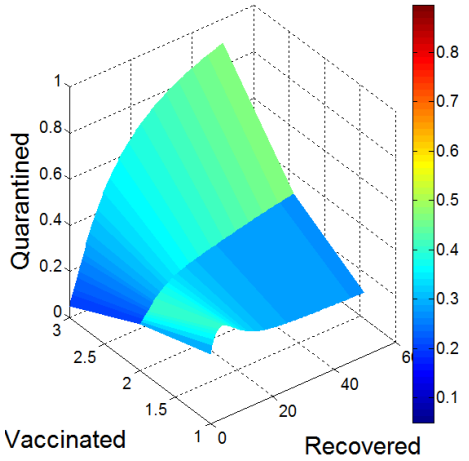

(b) Surface plot of the Vaccinated and Recovery measures on the Quarantined class

Figure 9. Human Population

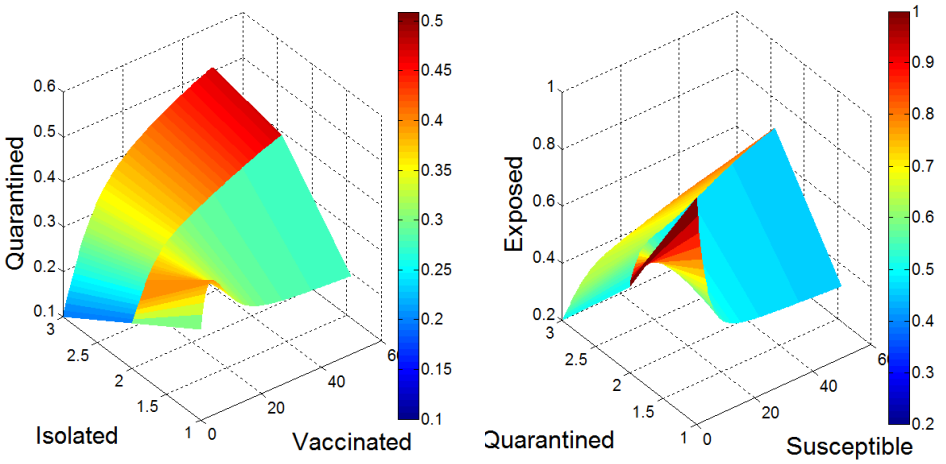

(a) Surface plot of the Isolated for treatment and Vaccination measures on the Quarantined class

(b) Surface plot of the Quarantined and Susceptible classes on the Exposed class

Figure 10. Total Human Population

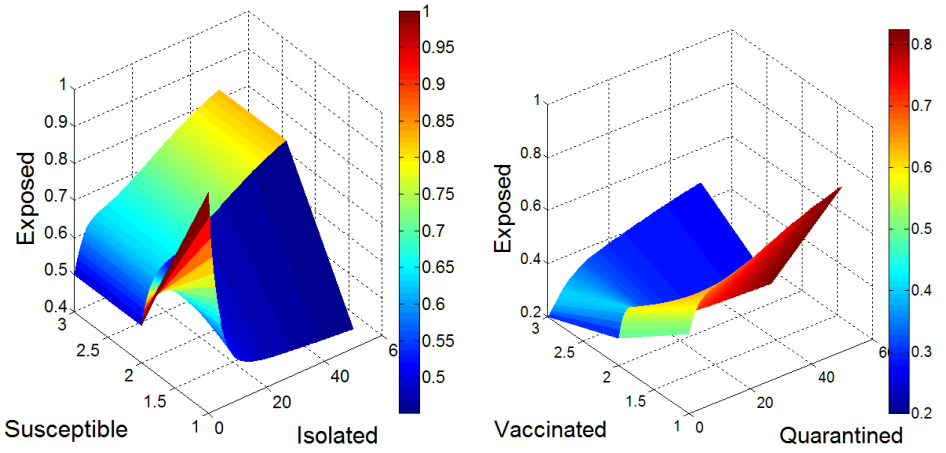

(a) Surface plot of the Susceptible and Isolated classes on the Exposed class

(b) Surface plot of the Quarantined and Vaccinated classes on the Exposed class

Figure 11. Human Population

to a pronounced reduction in the susceptible population. This behavior can be attributed to the intensified transition of individuals from the susceptible class into the vaccinated class and those exposed to COVID-19, reflecting the effectiveness of enhanced vaccination efforts and disease exposure dynamics. Concurrently, the exposed population rises as higher fractional orders facilitate faster transitions of susceptible individuals due to increased contact rates or improved vaccination outreach. This dynamic highlights the critical role of fractional-order models in capturing the memory effects and nonlocal dynamics that are characteristic of real-world epidemiological processes. Interestingly, a marginal rebound in the susceptible class is observed, which may be explained by two pivotal factors: the waning immunity of vaccinated individuals and the re-susceptibility of recovered individuals. The latter underscores the importance of maintaining vaccination boosters and post-recovery monitoring programs to mitigate the risk of reinfection. These findings emphasize the delicate balance between vaccination efficacy, natural immunity, and population susceptibility in controlling disease transmission.

Over time as $(t \to \infty)$, the exposed population steadily decreases as a result of targeted quarantine measures, which effectively reduce the likelihood of disease transmission from individuals in the latent stage of infection. These individuals are subsequently moved to the isolated class for treatment, thereby causing a corresponding decrease in the quarantined population. The isolated class, on the other hand, initially increases as more individuals transition from both the exposed and quarantined compartments. However, this increase is not permanent, as the isolated population eventually diminishes when patients recover under proper medical care. This trend underscores the pivotal role of health care infrastructure in managing disease spread, as well as the significance of providing timely medical interventions in isolation facilities. Furthermore, while the recovered population increases during the early phases due to successful treatments, it eventually declines due to the phenomenon of re-susceptibility, where recovered individuals lose immunity and become vulnerable to reinfection. This finding emphasizes the need for sustained public health vigilance, especially during subsequent phases of the pandemic, to prevent recurring surges in infection rates. For instance, ensuring that recovered individuals receive booster vaccinations or regular health screenings could help mitigate this decline in immunity over time. Figure (8(a)) corroborates these observations, highlighting how increased interactions between susceptible and exposed individuals contribute significantly to the rise in cumulative new cases of the disease. This result suggests that stricter measures, such as reducing contacts through social distancing, widespread testing, and early detection of exposed individuals, are critical for controlling cumulative case counts. Taken together, these findings emphasize that a holistic approach—combining quarantine, isolation, vaccination, and ongoing monitoring—is essential to managing COVID-19 transmission effectively.

The graph in Figure (8(b)) illustrates the prevalence rate of the modeled disease over time for different values of the parameter α_1, which governs the progression from the exposed compartment (E) to the isolated for treatment compartment (I_T). The prevalence rate, defined as the proportion of the total population affected by the disease (E + I_T + R) at any given time, is a key indicator of the disease burden within the population and provides critical insight into both the spread and control of the disease. The curves demonstrate how variations in α_1 impact the prevalence rate, with higher values of α_1 generally resulting in a higher initial prevalence but potentially faster isolation and treatment, thereby influencing the dynamics of dis-

ease control. This suggests that adjusting the progression from exposed to isolated individuals can be a vital strategy in controlling the disease's spread, with faster isolation leading to a quicker reduction in the number of infectious individuals. This type of analysis is essential in epidemiology for understanding the effects of intervention strategies and the progression of the disease under various scenarios.

Figure (5(b)) demonstrates that increasing the vaccination rate leads to a reduction in the number of individuals susceptible to COVID-19 and a corresponding increase in the number of recovered individuals, as depicted in Figure (6(a)). This highlights the direct impact of vaccination on reducing the pool of susceptible individuals and promoting immunity within the population. Similarly, Figure (6(b)) illustrates that a higher quarantine rate for exposed individuals decreases the exposed population, thereby mitigating the spread of the disease from latently infected individuals. This finding emphasizes the critical role of timely quarantine interventions in preventing outbreaks from escalating. This finding underscores the importance of enhancing quarantine facilities to ensure early detection of asymptomatic carriers. Moreover, Figure (7(a)) shows that increasing the provision of isolation centers reduces the number of individuals exposed to COVID-19. This reduction in exposure underscores the significance of isolation centers in limiting transmission, especially in high-risk areas. Isolation centers are crucial for separating infected individuals from those who are susceptible, thus preventing further transmission and facilitating recovery. Finally, Figure (7(b)) indicates that bolstering preventive measures, such as isolation, vaccination, and quarantine, leads to a substantial increase in the number of recovered individuals. This suggests that an integrated approach to disease control, combining all three strategies, can significantly enhance recovery rates.

The surface plot in Figure (9(a)) demonstrates that combining quarantine and isolation measures can significantly reduce the cumulative new cases of COVID-19 in the population, maintaining the cumulative incidence below one. This highlights the importance of a comprehensive approach to disease control, as the combination of these measures effectively reduces transmission and overall incidence. This finding underscores the effectiveness of fully implementing these measures to lower the prevalence of COVID-19. Figure (9(b)) illustrates that enhancing vaccination efforts and increasing the recovery rate of infected individuals will decrease the number of people in the quarantined class, primarily composed of individuals exposed to the disease. This emphasizes the importance of proactive vaccination strategies and timely recovery interventions in reducing the burden on quarantine systems. This ensures that the quarantined population remains below one. Similarly, increasing the isolation rate of infected individuals for treatment and the vaccination rate of susceptible individuals will further reduce the quarantined population, maintaining it below one. These measures, when combined, offer a robust strategy for minimizing the spread of the disease. The combined effects of quarantine, isolation, and vaccination measures, as shown in Figures (10(b)), (11(a)), and (11(b)), result in a decrease in the population exposed to COVID-19, thereby reducing the overall prevalence of the disease in the population. The interaction of these strategies reveals how targeted interventions can effectively limit the disease spread and facilitate control over time. These findings highlight the critical importance of a multifaceted approach in controlling and mitigating the spread of COVID-19.

5. Conclusion

In conclusion, we investigated the role of vaccination, quarantine and isolating the infected for treatment in reducing the transmission of the corona virus by analyzing a system of six nonlinear fractional-order equations in the Caputo sense.

The suggested coronavirus model under three different control measures namely (vaccination, quarantine and isolation) was shown to exist and to have unique solutions using the Schauder and Banach fixed point theorems, respectively. Ulam-Hyers and generalized Ulam-Hyers stability analysis frameworks were developed. The fractional Euler method is a first-order convergent numerical methodology that was used to numerically simulate the fractional variation of the model under discussion via the Caputo fractional operator.

With the fractional-order number , we illustrated the profiles of every variable under the Caputo fractional derivative. The dynamical outlook of each variable was examined and illustrated for varying fractional-order values. The results underscore the effectiveness of higher vaccination rates, enhanced quarantine measures, and improved isolation facilities in reducing COVID-19 transmission. The model shows that these actions not only decrease susceptibility and exposure but also accelerate recovery, significantly limiting disease spread. Ultimately, integrating these control measures is crucial for effectively managing and containing COVID-19 outbreaks.

Funding
No funding was received.

Availability of data
Values of parameters used are adequately cited and referenced.

Competing Interests
The authors declare no conflict of interest.

Credit authorship contribution statement
Remigius Aja Okeke wrote the original draft; **William Atokolo** conducted formal analysis; **David Omale** provided supervision, **Godwin Onuche Acheneje** contributed to software development and reviewed the work; **Jeremiah Amos** participated in review and editing, and **Agbata Celestine** also contributed to the review.

References

[1] World Health Organization, *Report of the WHO-China joint mission on coronavirus disease 2019 (COVID-19)*, 2020.
https://www.who.int/docs/defaultsource/coronaviruse/who-china-joint-mission-on-covid-19-final-report.pdf

[2] World/Countries/Pakistan, *Total Coronavirus Cases in Pakistan*, Available online: https://www.worldometers.info/coronavirus/country/pakistan/

[3] S. Khajanchi, K. Sarkar, S. Banerjee, *Modeling the dynamics of COVID-19 pandemic with implementation of intervention strategies*, Eur. Phys. J. Plus 137, 1–22, 2022.
DOI: 10.1140/epjp/s13360-022-01610-3

[4] M.S. Ullah, M. Higazy, K.A. Kabir, *Modeling the epidemic control measures in overcoming COVID-19 outbreaks: A fractional-order derivative approach*, Chaos Solitons Fractals 155, 111636, 2022.
DOI: 10.1016/j.chaos.2022.111636

[5] A. Cioffi, F. Cioffi, *COVID-19 vaccine: Risk of inequality and failure of public health strategies*, Ethics Med. Public Health 17, 100653, 2021.
DOI: 10.1016/j.jemp.2021.100653

[6] Q. Zheng, X. Wang, C. Bao, Y. Ji, H. Liu, Q. Meng, Q. Pan, *A multi-regional, hierarchical-tier mathematical model of the spread and control of COVID-19 epidemics from epicentre to adjacent regions*, Transbound. Emerg. Dis. 69, 549–558, 2022.
DOI: 10.1111/tbed.14111

[7] J. Deng, S. Tang, H. Shu, *Joint impacts of media, vaccination and treatment on an epidemic Filippov model with application to COVID-19*, J. Theor. Biol. 523, 110698, 2021.
DOI: 10.1016/j.jtbi.2020.110698

[8] C. Chen, N.S. Chong, *A Filippov model describing the effects of media coverage and quarantine on the spread of human influenza*, Math. Biosci. 296, 98–112, 2018.
DOI: 10.1016/j.mbs.2017.11.007

[9] M.A. Acuña-Zegarra, S. Díaz-Infante, D. Baca-Carrasco, D. Olmos-Liceaga, *COVID-19 optimal vaccination policies: A modeling study on efficacy, natural and vaccine-induced immunity responses*, Math. Biosci. 337, 108614, 2021.
DOI: 10.1016/j.mbs.2020.108614

[10] A. Omame, R. Umana, D. Okuonghae, S. Inyama, *Mathematical analysis of a two-sex Human Papillomavirus (HPV) model*, Int. J. Biomath. 11, 1850092, 2018.
DOI: 10.1142/S1793524518500923

[11] E. Elbasha, C. Podder, A. Gumel, *Analyzing the dynamics of an SIRS vaccination model with waning natural and vaccine-induced immunity*, Nonlinear Anal. Real World Appl. 12, 2692–2705, 2011.
DOI: 10.1016/j.nonrwa.2011.04.014

[12] P. Doutor, P. Rodrigues, M.d.C. Soares, F.A. Chalub, *Optimal vaccination strategies and rational behaviour in seasonal epidemics*, J. Math. Biol. 73, 1437–1465, 2016.
DOI: 10.1007/s00285-016-0986-4

[13] H. Laarabi, M. Rachik, O. El Kahlaoui, E. Labriji, *Optimal vaccination strategies of an SIR epidemic model with a saturated treatment*, Univers. J. Appl. Math. 1, 185–191, 2013.
DOI: 10.20286/ujam.2013.01018

[14] M. Parsamanesh, R. Farnoosh, *On the global stability of the endemic state in an epidemic model with vaccination*, Math. Sci. 12, 313–320, 2018.
DOI: 10.1007/s40096-017-0263-6

[15] M. Parsamanesh, M. Erfanian, S. Mehrshad, *Stability and bifurcations in a discrete-time epidemic model with vaccination and vital dynamics*, BMC Bioin-

form. 21, 1–15, 2020.
DOI: 10.1186/s12859-020-03559-3

[16] X. Han, H. Liu, X. Lin, Y. Wei, M. Ming, *Dynamic Analysis of a VSEIR Model with Vaccination Efficacy and Immune Decline*, Adv. Math. Phys., 2022.
DOI: 10.1155/2022/3212547

[17] M.A. Khan, A. Atangana, *Modeling the dynamics of novel coronavirus (2019-nCov) with fractional derivative*, Alex. Eng. J. 59, 2379–2389, 2020.
DOI: 10.1016/j.aej.2020.06.013

[18] M.A. Khan, A. Atangana, E. Alzahrani, *The dynamics of COVID-19 with quarantined and isolation*, Adv. Differ. Equ., 1–22, 2020.
DOI: 10.1186/s13662-020-00250-0

[19] M.A.A. Oud, A. Ali, H. Alrabaiah, S. Ullah, M.A. Khan, S. Islam, *A fractional order mathematical model for COVID-19 dynamics with quarantine, isolation, and environmental viral load*, Adv. Differ. Equ., 1–19, 2021.
DOI: 10.1186/s13662-021-00296-1

[20] F. Rihan, H. Alsakaji, *Dynamics of a stochastic delay differential model for COVID-19 infection with asymptomatic infected and interacting people: Case study in the UAE*, Results Phys. 28, 104658, 2021.
DOI: 10.1016/j.rinp.2021.104658

[21] N. Anggriani, M.Z. Ndii, R. Amelia, W. Suryaningrat, M.A.A. Pratama, *A mathematical COVID-19 model considering asymptomatic and symptomatic classes with waning immunity*, Alex. Eng. J. 61, 113–124, 2022.
DOI: 10.1016/j.aej.2022.05.015

[22] X. Liu, S. Ullah, A. Alshehri, M. Altanji, *Mathematical assessment of the dynamics of novel coronavirus infection with treatment: A fractional study*, Chaos Solitons Fractals 153, 111534, 2021.
DOI: 10.1016/j.chaos.2021.111534

[23] A. Beigi, A. Yousefpour, A. Yasami, J. Gómez-Aguilar, S. Bekiros, H. Jahanshahi, *Application of reinforcement learning for effective vaccination strategies of coronavirus disease 2019 (COVID-19)*, Eur. Phys. J. Plus 136, 1–22, 2021.
DOI: 10.1140/epjp/s13360-021-01971-1

[24] R. Martinez-Guerra, J.P. Flores-Flores, *An algorithm for the robust estimation of the COVID-19 pandemics population by considering undetected individuals*, Appl. Math. Comput. 405, 126273, 2021.
DOI: 10.1016/j.amc.2021.126273

[25] M.A. Khan, S. Ullah, S. Kumar, *A robust study on 2019-nCOV outbreaks through non-singular derivative*, Eur. Phys. J. Plus 136, 1–20, 2021.
DOI: 10.1140/epjp/s13360-021-01722-1

[26] M.A. Khan, A. Atangana, *Mathematical modeling and analysis of COVID-19: A study of new variant Omicron*, Phys. A Stat. Mech. Its Appl. 599, 127452, 2022.
DOI: 10.1016/j.physa.2022.127452

[27] A. Muniyappan, B. Sundarappan, P. Manoharan, M. Hamdi, K. Raahemifar, S. Bourouis, V. Varadarajan, *Stability and numerical solutions of second wave mathematical modeling on covid-19 and omicron outbreak strategy of pandemic:*

Analytical and error analysis of approximate series solutions by using hpm, Mathematics 10, 343, 2022.
DOI: 10.3390/math10040343

[28] P. Pandey, J. Gómez-Aguilar, M.K. Kaabar, Z. Siri, A.M. Abd Allah, *Mathematical modeling of COVID-19 pandemic in India using Caputo-Fabrizio fractional derivative*, Comput. Biol. Med. 145, 105518, 2022.
DOI: 10.1016/j.compbiomed.2022.105518

[29] G.O. Acheneje, D. Omale, B.C. Agbata, W. Atokolo, M.M. Shior, B. Bolarinwa, *Approximate Solution of the Fractional Order Mathematical Model on the Transmission Dynamics on The Co-Infection of COVID-19 and Monkeypox Using the Laplace-Adomian Decomposition Method*, International Journal of Mathematics and Statistics Studies, 12(3), 17–51, 2024.
DOI: 10.37745/ijmss.13/vol12n31751

[30] C. Zhang, R.P. Agarwal, M. Bohner, T. Li, *Oscillation of second-order nonlinear neutral dynamic equations with noncanonical operators*, Bull. Malays. Math. Sci. Soc. 38, 761–778, 2015.
DOI: 10.1007/s40840-018-0610-6

[31] S. Chen, Q. Zhao, Y. Ye, B. Qu, *Using IIR filter in fractional order phase lead compensation PIMR-RC for grid-tied inverters*, IEEE Trans. Ind. Electron., 1–10, 2022.
DOI: 10.1109/TIE.2022.3206463

[32] M. Areshi, A.R. Seadawy, A. Ali, A.F. Alharbi, A.F. Aljohani, *Analytical Solutions of the Predator-Prey Model with Fractional Derivative Order via Applications of Three Modified Mathematical Methods*, Fractal Fract. 7, 1–14, 2023.
DOI: 10.3390/fractalfract7010001

[33] X. Wu, S. Wen, W. Shao, J. Wang, *Numerical Investigation of Fractional Step-Down ELS Option*, Fractal Fract. 7, 126, 2023.
DOI: 10.3390/fractalfract7010010

[34] Y. He, Z. Wang, *Stability analysis and optimal control of a fractional cholera epidemic model*, Fractal Fract. 6, 157, 2022.
DOI: 10.3390/fractalfract6010008

[35] I.A. Baba, U.W. Humphries, F. Rihan, *Role of Vaccines in Controlling the Spread of COVID-19: A Fractional-Order Model*, Vaccines 11, 145, 2023.
DOI: 10.3390/vaccines11020145

[36] S. Okyere, J. Ackora-Prah, *Modeling and analysis of monkeypox disease using fractional derivatives*, Results Eng. 17, 100786, 2023.
DOI: 10.1016/j.rinp.2023.100786

[37] W. Atokolo, R.O. Aja, S.E. Aniaku, I.S. Onah, G.C.E. Mbah, *Approximate solution of the fractional order sterile insect Technology model via the Laplace Adomian Decomposition method for the spread of Zika virus Disease*, Int. J. Math. Math. Sci., Article ID 2297630, 2022.
DOI: 10.1155/2022/2297630

[38] W. Atokolo, R.O. Aja, D. Omale, Q.O. Ahmon, G.O. Acheneje, J. Amos, *Fractional mathematical model for the transmission dynamics and control of Lassa fever*, Franklin Open, Article ID 100110, 2024.
DOI: 10.1016/j.fraope.2024.100110

[39] M. Akter, M. Nurunnahar, M.Z. Ullah, A.A. Meetei, A.M. Zaagan, A.M. Mahnashi, *An innovative fractional-order evolutionary game theoretical study of personal protection, quarantine, and isolation policies for combating epidemic diseases*, Scientific Reports, 2024.
DOI: 10.1038/s41598-024-61211-2

[40] M. Ullah, K.M.A. Kabir, *Behavioral game of quarantine during the monkeypox epidemic: Analysis of deterministic and fractional order approach*, Heliyon, 2024.
DOI: 10.1016/j.heliyon.2024.e26998

[41] M. Ullah, K. M. A. Kabir, Md. Abdul, H. Khan, *A non-singular fractional-order logistic growth model with multi-scaling effects to analyze and forecast population growth in Bangladesh*, Scientific Reports, 2023.
DOI: 10.1038/s41598-023-45773-1

[42] M. Ullah, M. Higazy, K. Kabir, *Dynamic analysis of mean-field and fractional-order epidemic vaccination strategies by evolutionary game approach*, Chaos, Solitons & Fractals, 2022.
DOI: 10.1016/j.chaos.2022.112431

[43] M. S. Ullah, M. Kamrujjaman, K. M. A. Kabir, *Understanding the relationship between stay-at-home measures and vaccine shortages: A conventional, heterogeneous, and fractional dynamic approach*, J Health Popul Nutr, 43(1):32, 2024.
DOI: 10.1186/s41043-024-00505-7

[44] M. Parsamanesh, M. Erfanian, *Global dynamics of an epidemic model with standard incidence rate and vaccination strategy*, Chaos, Solitons & Fractals, 2018.
DOI: 10.1016/J.CHAOS.2018.10.022

[45] X. Liu, S. Ullah, A. Alshehri, M. Altanji, *Mathematical assessment of the dynamics of novel coronavirus infection with treatment: A fractional study*, Chaos, Solitons & Fractals, 2021.
DOI: 10.1016/j.chaos.2021.111534

[46] M. Bachar, M. Khamsi, M. Bounkhel, *A mathematical model for the spread of COVID-19 and control mechanisms in Saudi Arabia*, Advances in Difference Equations, 2021.
DOI: 10.1186/s13662-021-03410-z

[47] M. Parsamanesh, M. Erfanian, *Stability and bifurcations in a discrete-time SIVS model with saturated incidence rate*, Chaos, Solitons & Fractals, 2021.
DOI: 10.1016/J.CHAOS.2021.111178

[48] H. Gholami, M. Gachpazan, M. Erfanian, *SEIaIsQRS epidemic model for COVID-19 by using compartmental analysis and numerical simulation*, Computational Modeling in Differential Equations, 2024.
DOI: 10.22034/cmde.2024.58656.2482

[49] V. Pata, *Fixed point theorems and applications*, Dipartmentso di matematica "F.Briuschi" politecnico di Milano.
URL: https://www.karlin.mff.cunbcz

[50] H. Zou, *Handbook of Differential Equations stationary partial Differential Equations*, 2008.

[51] H. Jinghao, Y. Huang, Y. Li, *Hyers-Ulam stability of linear functional differential equations*, J. Math. Anal. Appl., 2015.
DOI: 10.1016/j.jmaa.2015.02.018

[52] S. Ciplea, N. Lungu, *On Ulam-Hyers Stability for a System of Partial Differential Equations of First Order*, Symmetry, 12:1060, 2020.
DOI: 10.3390/sym12071060

[53] A. Kilbas, H. Srivastava, J. Trujillo, *Theory and Applications of Fractional Differential Equations*, North-Holland Mathematics Studies, vol. 204, 2006.

[54] M. S. Abdo, K. Shah, H. A. Wahash, S. K. Panchal, *On a comprehensive model of the novel coronavirus (COVID-19) under Mittag-Leffler derivative*, Chaos Solitons Fractals, 135:109867, 2020.
DOI: 10.1016/j.chaos.2020.109867

[55] K. Shah, T. Abdeljawad, I. Mahariq, F. Jarad, *Qualitative analysis of a mathematical model in the time of COVID-19*, BioMed Res. Int., Article ID 5098598, 2020.
DOI: 10.1155/2020/5098598

[56] H. Khan, Y. Li, A. Khan, A. Khan, *Existence of solution for a fractional-order Lotka-Volterra reaction-diffusion model with Mittag-Leffler kernel*, Math. Methods Appl. Sci., 42:3377-3387, 2019.
DOI: 10.1002/mma.5618

[57] H. Khan, T. Abdeljawad, M. Aslam, R. A. Khan, A. Khan, *Existence of positive solution and Hyers-Ulam stability for a nonlinear singular-delay-fractional differential equation*, Adv. Differ. Equ., Article ID 104, 2019.
DOI: 10.1186/s13662-019-2325-8

[58] A. Khan, J. Gómez-Aguilar, T. S. Khan, H. Khan, *Stability analysis and numerical solutions of fractional order HIV/AIDS model*, Chaos Solitons Fractals, 122:119-128, 2019.
DOI: 10.1016/j.chaos.2019.02.007

[59] A. Khan, J. Gómez-Aguilar, T. Abdeljawad, H. Khan, *Stability and numerical simulation of a fractional order plant-nectar-pollinator model*, Alex. Eng. J., 59:49-59, 2020.
DOI: 10.1016/j.aej.2019.12.006

[60] S. M. Ulam, *A Collection of Mathematical Problems*, vol. 8, Interscience, New York, 1960.

[61] S. M. Ulam, *Problems in Modern Mathematics*, Courier Corporation, 2004.

[62] I. Ahmed, P. Kumam, K. Shah, P. Borisut, K. Sitthithakerngkiet, M. A. Demba, *Stability results for implicit fractional pantograph differential equations via ϕ-Hilfer fractional derivative with a nonlocal Riemann-Liouville fractional integral condition*, Mathematics, 8:94, 2020.
DOI: 10.3390/math8010094

[63] I. Ahmed, P. Kumam, F. Jarad, P. Borisut, K. Sitthithakerngkiet, A. Ibrahim, *Stability analysis for boundary value problems with generalized nonlocal condition via Hilfer-Katugampola fractional derivative*, Adv. Differ. Equ., Article ID 225, 2020.
DOI: 10.1186/s13662-020-02731-8

[64] Z. Ali, P. Kumam, K. Shah, A. Zada, *Investigation of Ulam stability results of a coupled system of nonlinear implicit fractional differential equations*, Mathematics, 7:341, 2019.
DOI: 10.3390/math7040341

[65] A. Aphithana, S. K. Ntouyas, J. Tariboon, *Existence and Ulam-Hyers stability for Caputo conformable differential equations with four-point integral conditions*, Adv. Differ. Equ., Article ID 139, 2019.
DOI: 10.1186/s13662-019-2116-2

[66] A. Khan, H. Khan, J. Gómez-Aguilar, T. Abdeljawad, *Existence and Hyers-Ulam stability for a nonlinear singular fractional differential equations with Mittag-Leffler kernel*, Chaos Solitons Fractals, 127:422-427, 2019.
DOI: 10.1016/j.chaos.2019.07.026

[67] C. Li, F. Zeng, *Numerical Methods for Fractional Calculus*, vol. 24, CRC Press, Boca Raton, 2015.
DOI: 10.1201/b18503

[68] D. Baleanu, A. Jajarmi, M. Hajipour, *On the nonlinear dynamical systems within the generalized fractional derivatives with Mittag-Leffler kernel*, Nonlinear Dyn., 94(1):397-414, 2018.
DOI: 10.1007/s11071-018-4367-y

[69] A. Jajarmi, D. Baleanu, *A new fractional analysis on the interaction of HIV with $CD4^+$ T-cells*, Chaos Solitons Fractals, 113:221-229, 2018.
DOI: 10.1016/j.chaos.2018.06.009

[70] A.K. Misra, A. Sharma, J. Shukla, *Modeling and analysis of effects of awareness programs by media on the spread of infectious diseases*, Math. Comput. Model., 53(5-6):1221-1228, 2011.
DOI: 10.1016/j.mcm.2010.12.005

[71] M. Tahir, S. I. A. Shah, G. Zaman, T. Khan, *A dynamic compartmental mathematical model describing the transmissibility of MERS-CoV virus in public*, Punjab Univ. J. Math., 51:57-71, 2019.

[72] National Population Commission, ICF Macro, *Nigeria Demographic and Health Survey 2008*, National Population Commission and ICF Macro, Abuja, 2009.